2 and 3.- Observations of the corona and Solar Wind

1) Density determination in the corona

- Separation of K continuum (photospheric light scattered by free electrons polarized) from the F continuum (photospheric light scattered by dust particles ; not significantly polarized near Sun) by photopolarimetric observations of corona during eclipses.

- Assuming radially symmetric and homogenous electron density model, $N_e(r)$ deduce theoretical brightness distribution. - Compare with observations - correct $N_e(r)$ model - deduce new theoretical brightnesses ... etc ...

$$N_e(r) = \sum_n a_n r^{-n}$$

$$N_e(1{,}5\ R_\odot) \simeq 10^7\ cm^{-3}$$

- Fig. 1
- Alpha particle concentration (not well known)

$$N_{\alpha++}/N_{p^+} \simeq 0.1\ (?)$$

- Proton particle concentration (from quasi-neutrality eq.)

$$N_p + 2\ N_\alpha = N_e \quad ; \quad N_p \simeq 0.83\ N_e$$

- $N_e(r, \theta, \varphi)$, depends on colatitude θ and heliocentric longitude φ (Streamers broadening of apparent diameter of Radio Source; Radio source scintillation)

$$X = \langle N_e^2 \rangle / \langle N_e \rangle^2$$

$$X(1{,}5\ R_\odot) \simeq 1.6\ \frac{r}{R_\odot} - 0.7$$

2) Determination of temperature in corona

- From isothermal barometric law

$$T_e = \frac{10^7 \mu}{\text{dlog } N_e/d(1/r)}$$

- dlog $N_e/d(1/r)$ determined from $N_e(r)$ (see above)

- μ mean molecular mass (= 608? if N_α/N_p = 0.1)

- $T_e(r)$ depends as $N_e(r)$ on solar activity

- $T_e(r)$ very sensitive to assumed value of X(r)

- T_e (1.5 $R_\odot$) = 2 x 10^6 K (confirmed by other methods : line broadening - degree of ionization - radio brightness temperature - Type III burst observations)

3) Determination of bulk velocities in corona

- By Radar Echos (38 Mc/S) at 1.6 $R_\odot$ in corona; Doppler shifts showed slow expansion (16 Km/sec) and erratic ("turbulent") motions ($\pm$ 100 km/sec)

4) Density measurements in interplanetary space

- with Faraday cups or/and curved surface electrostatic analysers, Energy per charge spectra are obtained (e.g. Fig. 2)

- $f(E) \sqrt{\frac{2E}{m}} \Delta E \propto J(>E_1/Q) - J(>E_2/Q)$

- N_p and $N_e = \int f(\vec{v})\, d\vec{v}$

- $N_e \approx N_p \in [\, 0.4\ cm^{-3};\ 80\ cm^{-3} \,]$

- $\langle N_p \rangle = 8.7 \pm 4\ cm^{-3}$

- Alpha particle distribution (e.g. Fig. 3)
  $N_\alpha / N_p = 0.045$ (comparable to photospheric abundance; higher values of N_α / N_p are usualy observed in high speed streams (≈ 0.25)

5) Velocities in interplanetary space

- $w = \sqrt{\dfrac{E_{max}/Q}{m/Q}}$

  E_{max}/Q value for which f(E/Q) is maximum (in energy spectra)

  $w \in [\, 200\ km/sec;\ 900\ km/sec \,]$ (e.g. Fig. 4)

- $\vec{w}$ approximately in radial direction ($\pm$ 10° - 15°)

- Quiet solar wind average: $\langle w \rangle = 325$ km/sec

- $w_{\alpha++} \approx w_{p+}$; $/(w_\alpha - w_p)/w_p < 15\%$ (e.g. Fig. 5)

6) Temperatures in interplanetary space

$$T_{\parallel,\perp} = \frac{m}{2k} \langle (\vec{v} - \langle \vec{w} \rangle)^2_{\parallel,\perp} \rangle$$

- $T_p = \dfrac{1}{3} (T_\parallel + 2\, T_\perp) \in [\, 5 \times 10^3 K;\ 10^6 K \,]$

- Temperature anisotropy in direction parallel to magnetic field $\vec{B}$;
  $(T_\parallel / T_\perp)_p \approx 2$ (e.g. Fig. 6)

- T_p correlated with proton bulk speed $\langle w_p \rangle$

$$\sqrt{\frac{T_p(K)}{10^3}} = 0.036 \langle v_p \rangle \text{ (km/sec)} - 5.54$$

(Burlaga and Ogilvie's relation) (Fig. 7)

- $\langle T_p \rangle = 4 \times 10^4$ K

- $\langle T_e \rangle = 1.5 \times 10^5$ K ; $(T_{\parallel}/T_{\perp})_e = 1.1$

- $T_\alpha \simeq 4\ T_p$; $(\bar{v}_\alpha \simeq \bar{v}_p)$

7) Magnetic field observations in interplanetary space

- 3 types of magnetometers (spin coil; flux gate magnetometer; nuclear spin precession magnetometer)

- $|\vec{B}| \in [\,0.25\ \gamma - 40\ \gamma\,]$ (Fig. 8)

  ($1\gamma = 10^{-5}$ Gauss) (N.F. Ness)

- $\langle |\vec{B}| \rangle = (6 \pm 0.5)\gamma$;

- $\langle \hat{B} \rangle$ // to ecliptic plane ; along Archemedian spatial direction, $\langle \phi_B \rangle = 135°$ or $315°$; (e.g. Fig. 9)

- $|B| \propto 4.13 \left[\frac{r(AU)}{1.5}\right]^{-1.25}$ (obs. radial dependance)

- Ness and Wilcox observed persistent sector structure during 3 solar rotations (Fig. 10)

- $\vec{B}$ at 1AU is correlated with $\vec{B}$ at photosphere (Fig. 11)

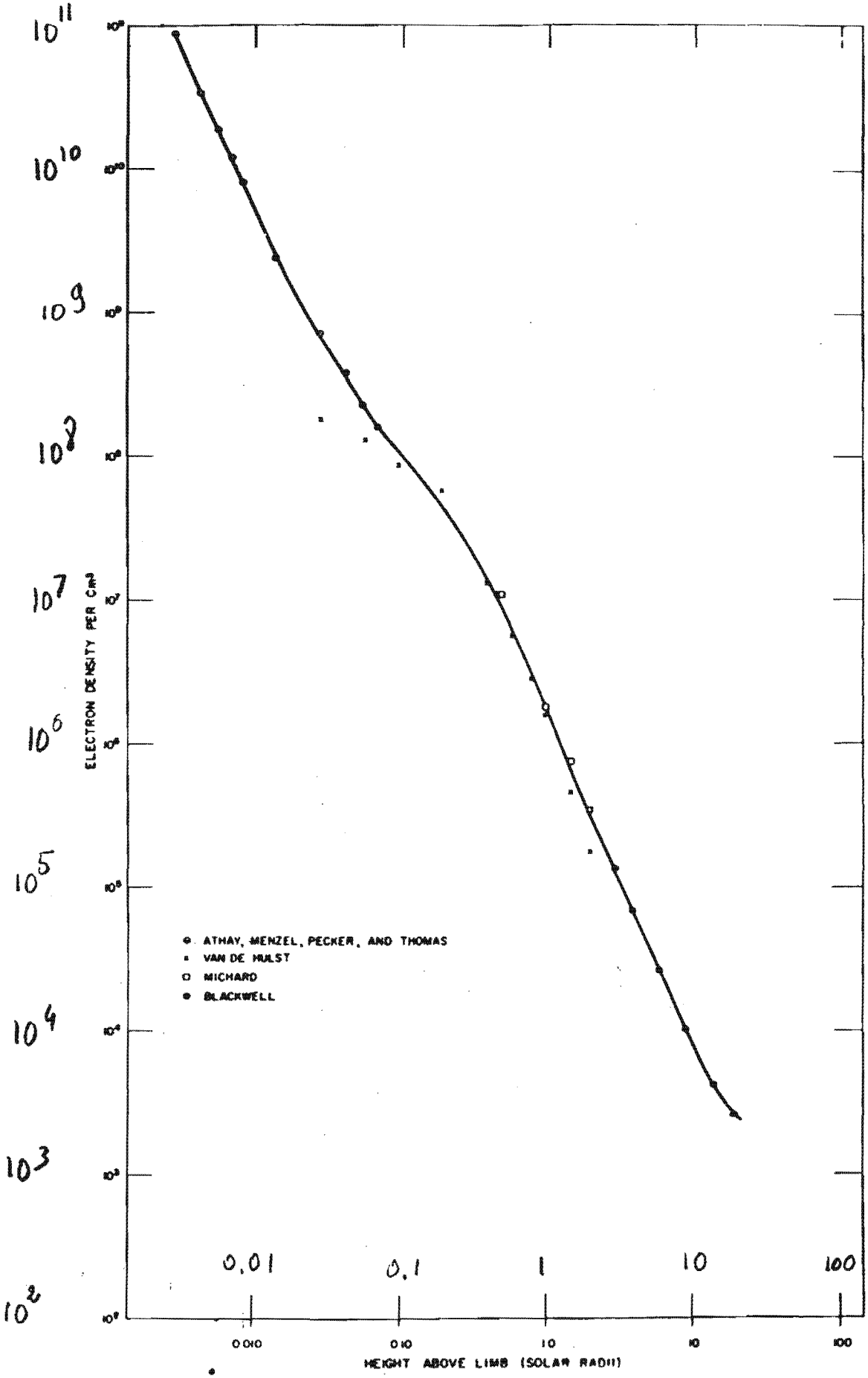

FIG. 1.—The electron density is plotted as a function of the height above the solar limb. The measures refer to the solar equator about the time of sunspot minimum.

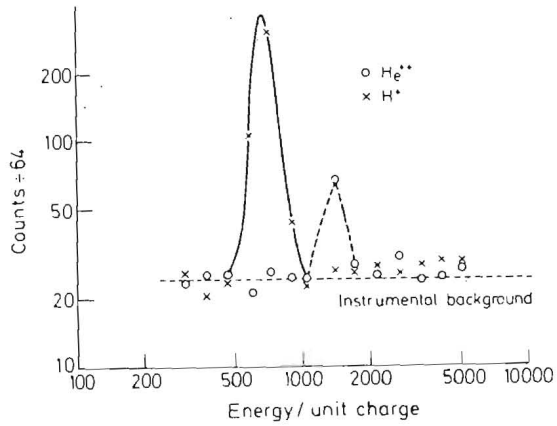

Fig. 2 Typical Explorer 34 energy-per-charge spectra at the mass to charge ratios $M/Q = 1$ and 2 atomic mass units per electronic charge. The first of these, corresponding to $^1H^+$, is indicated by the x's, while the second, corresponding to $^4He^{++}$, is indicated by the o's

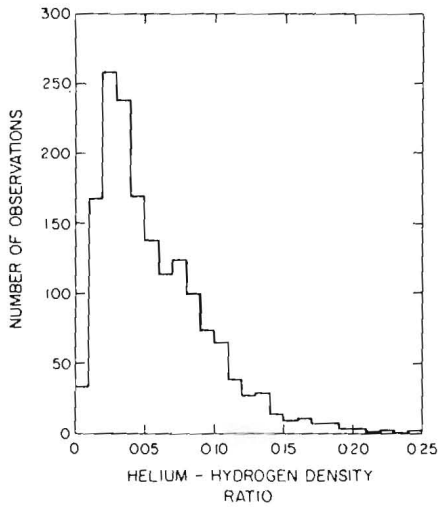

Fig. 3 The distribution of the ratios of helium and hydrogen number densities observed by the HEOS-1 satellite

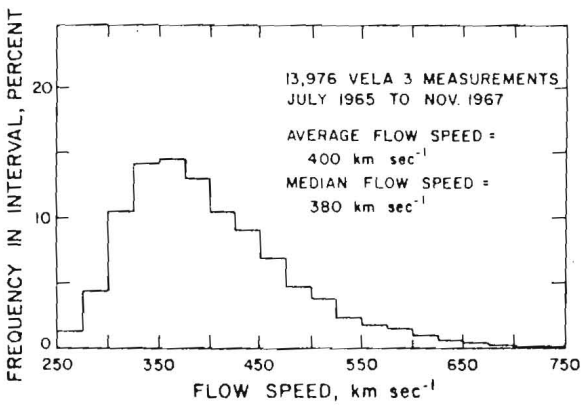

Fig. 4 A histogram of the flow speeds observed by Vela 3 spacecraft

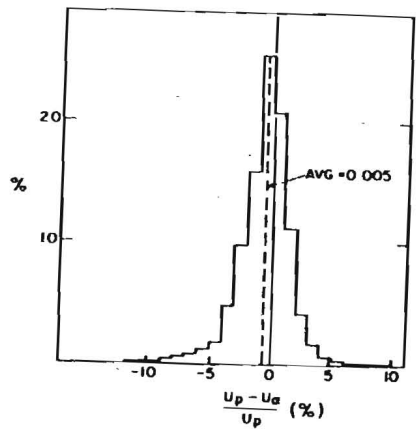

Fig. 5 Histograms of normalized bulk speed. (Top panel) All observations. (Bottom panel) All observations except for those taken in intervals A, B, and C of Figure 1.

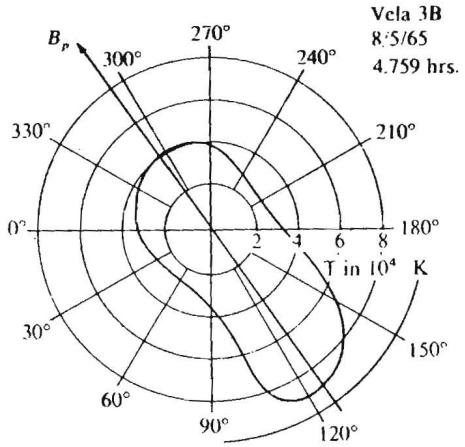

FIGURE 6

The temperature $T(\Phi)$ as defined by equation (5.1) is shown in the v_1v_2 plane for the distribution measured in Figure 5.5; the projected field B_p is also shown.

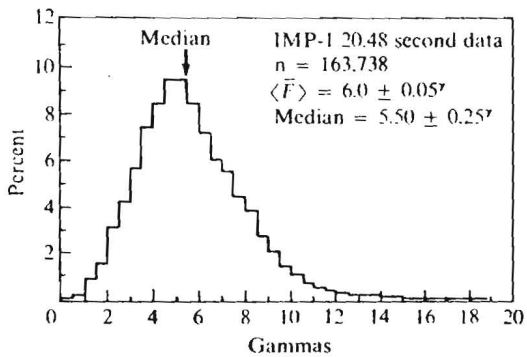

FIGURE 8

The distribution of interplanetary magnetic field magnitude as observed by IMP-I from 1963 to 1964.

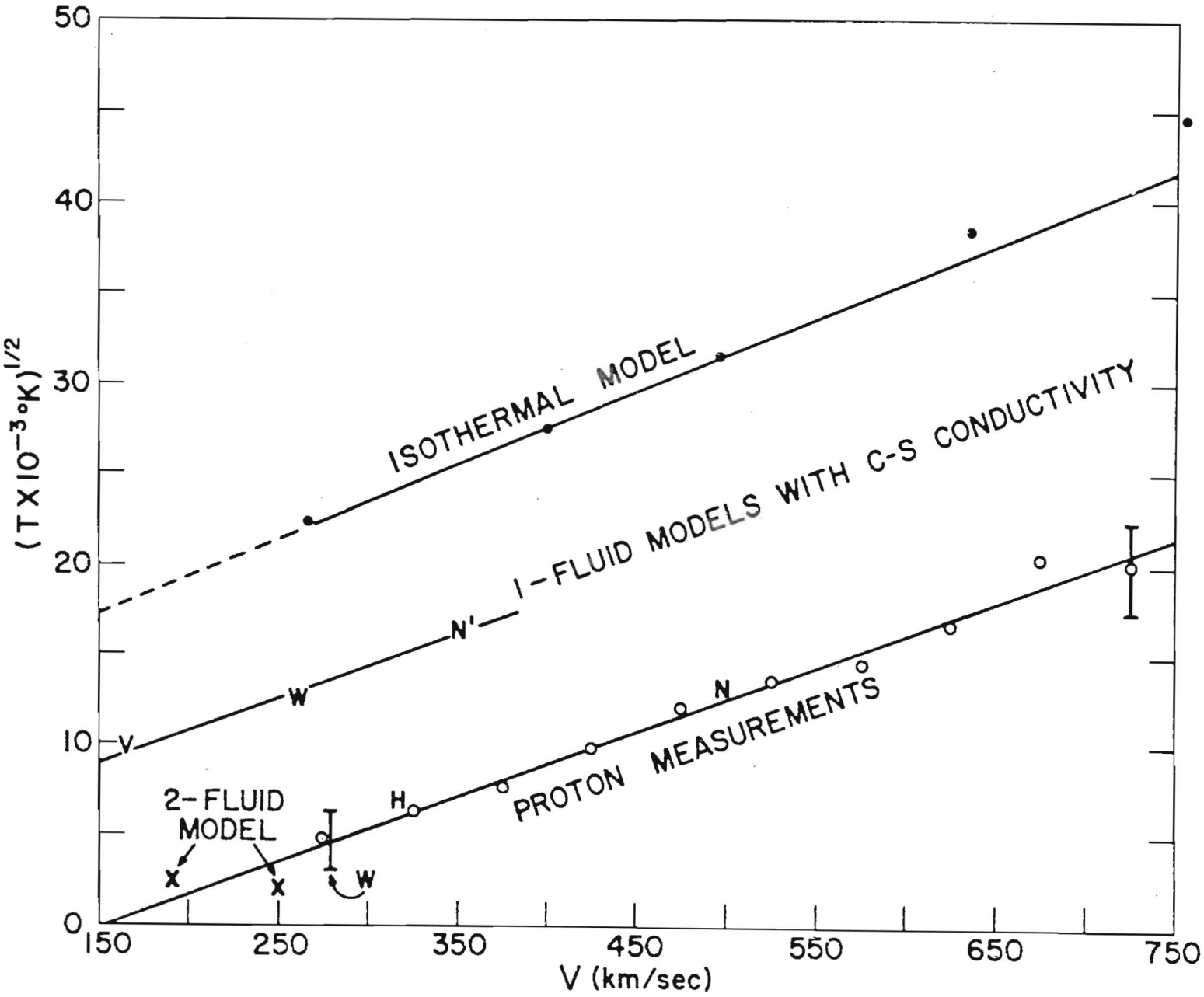
50
40
30
20
10
0
150
250
350
450
550
650
750
V (km/sec)
$(T \times 10^{-3} °K)^{1/2}$
ISOTHERMAL MODEL
1-FLUID MODELS WITH C-S CONDUCTIVITY
PROTON MEASUREMENTS
V
W
N'
N
H
2-FLUID MODEL
X
X
W

Figure 7

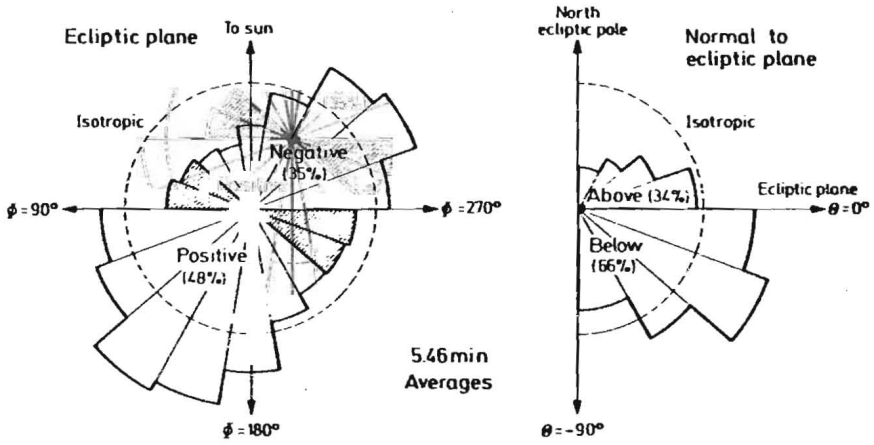

Fig 9 Histograms of the interplanetary magnetic field orientation observed on Imp 1 in 1963 [1]. The angle ϕ is the solar ecliptic longitude of the vector field (with $\phi = 0$ the direction toward the sun) and the angle θ is the solar ecliptic latitude of the vector field

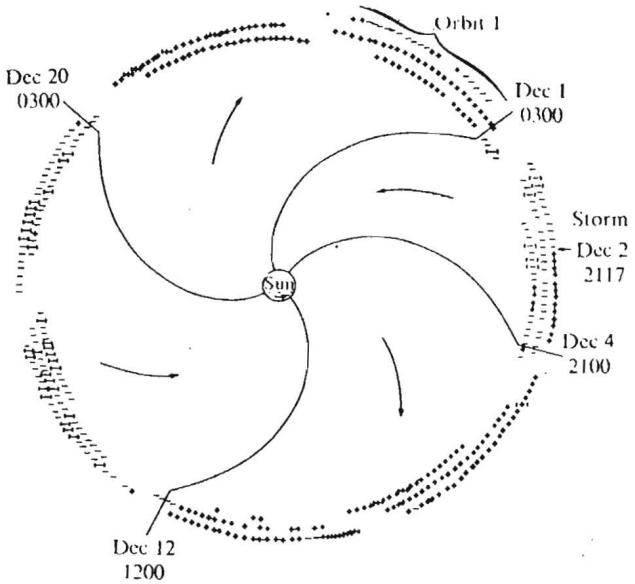

FIGURE 10
The sector structure of the interplanetary magnetic field observed by IMP-1. The plus or minus polarities correspond to the positive and negative directions indicated in Figure 5.11. Polarities in parentheses correspond to a movement into the shaded area of Figure 5.11 for a few hours in a smooth and continuous manner.

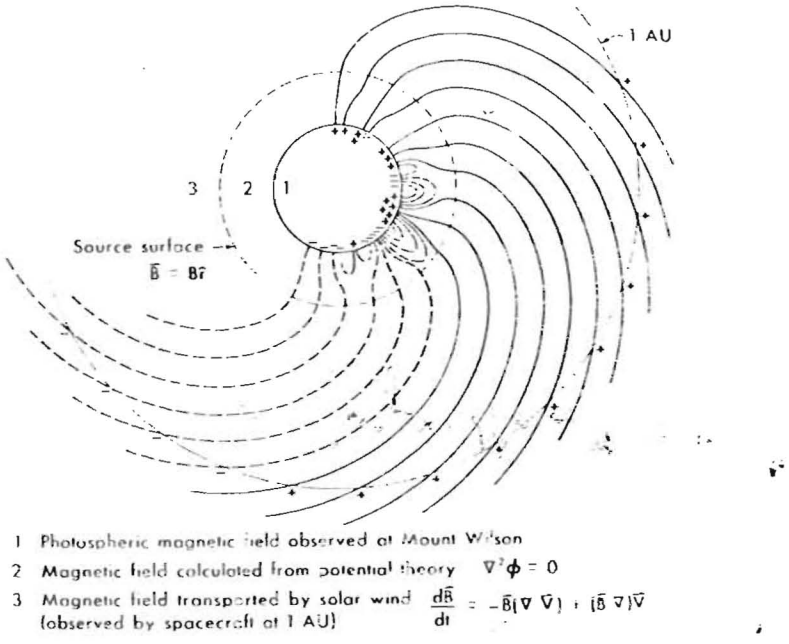

Fig. 11 A sketch illustrating the computation of the coronal magnetic field configuration in the "source surface" model

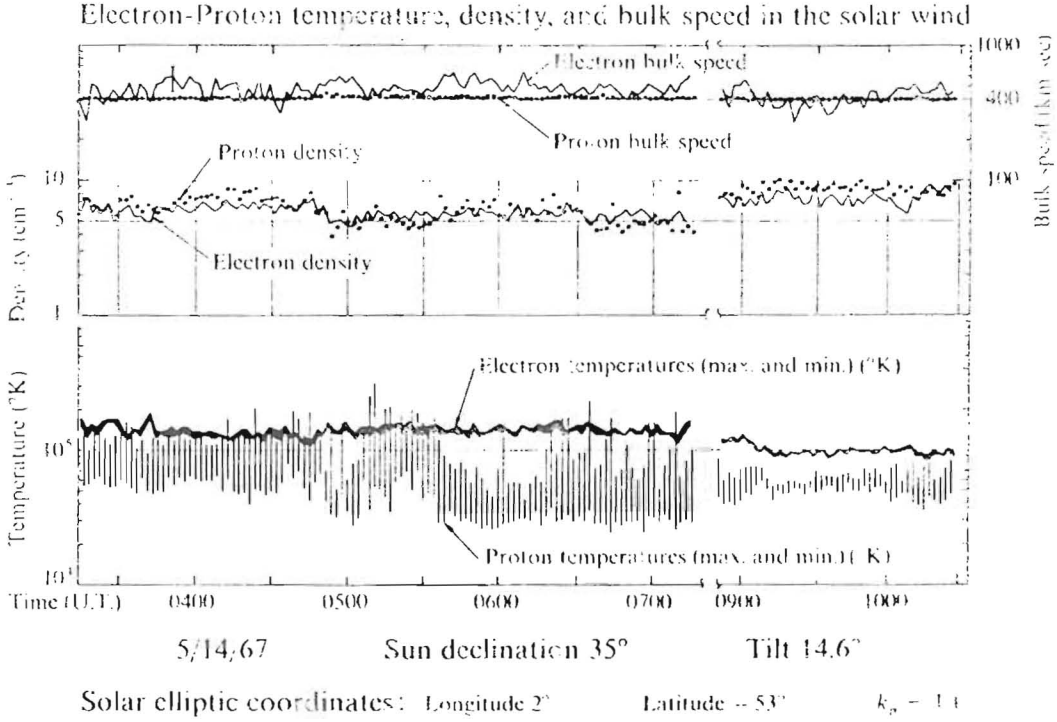

FIGURE 12

The proton and electron properties of the solar wind for a short length of time. The densities and velocities of protons and electrons are equal (to within the errors of measurement, but the temperature differences are significant.

3d Cycle Astronomy : The Solar Wind (3d lesson : J. LEMAIRE 28 oct. 1975)

Some characteristic distances, times and dimensionless numbers in the corona and solar wind

Heliocentric distance	$r\ [R_\odot = 6.96\ 10^{10}\ cm]$	1.5	215	$R_\odot$
Electron concentration	N_e	10^7	5	cm^{-3}
Helium abundance	$N_{\alpha++}/N_{p+}$	(10)	5	%
Electron temperature	T_e	2.10^6	$1.5\ 10^5$	K
Proton temperature	T_p	2.10^6	$4.\ 10^4$	K
Alpha temperature	T_α	(2.10^6)	$16.\ 10^4$	K
Bulk speed	w	(15)	325	km/s
Magnetic field	B	0.5	$5\ 10^{-5}$	Gauss
Thermal speed (p^+)	$v_T = \sqrt{2\ k\ T/m} = 0.128\ \sqrt{T[K]}/A$ [km/s]	182	25	km/s
Thermal speed (e^-)		7800	2130	km/s
Mach number	$\mathcal{M} = w/v_T = 8.5\ w\ [km/s]\ /\sqrt{T_e + T_p[K]}$	.06	9	---
Alfvèn speed	$v_A = \sqrt{B^2/4\pi\rho} = 21.5 \times 10^5\ B[G]\ /\sqrt{N_e\ [cm^{-3}]}$ [km/s]	330	48	km/s
Magnetic Mach number	$\mathcal{M}_m = w/v_A = 4.5\ 10^{-7}\ w(km/s)\ \sqrt{N_e[cm^{-3}]}/B\ [G]$	.05	6	---
Plasma oscillation period	$t_{Pl} = \frac{2\pi}{\omega_p} = \frac{2\pi\ m_e}{(4\pi\ N_e\ e^2)^{1/2}} = 10^{-4}/\sqrt{N_e[cm^{-3}]}$ [sec]	$3\ 10^{-3}$	$5\ 10^{-5}$	sec
Larmor period (p^+)	$t_L = \frac{2\pi mc}{Ze\ B} = 6\ 10^{-4}\ A/Z\ B\ [G]$ [sec]	10^{-3}	13	sec
(e^-)		$7\ 10^{-7}$	$7\ 10^{-3}$	sec
Close collision time (p^+)	$t_c = \frac{m^{1/2}\ (3\ k\ T)^{3/2}}{\sqrt{2}\ \pi\ e^4\ N} = 46\ A^{1/2}\ T^{3/2}/N_e\ [cm^{-3}]$ [sec]	10^4	$7\ 10^7$	sec

Deflection coll. time (e^-)	$t_D^e = \frac{\pi^2/4}{\langle X^2 \rangle} = \frac{\pi m_e^2 v^3}{32 N_e e^4 \ln \Lambda} = 2.6\ 10^{-2}\ T^{3/2}/N_e$ [sec]	7	$3\ 10^5$	sec
Deflection coll. time (p^+)	$t_D^p = \sqrt{m_p/m_e}\ \ t_D^e/\sqrt{2}$	220	10^6	sec
Energy equipartition time ($e^- p$)	$t_{eq} = \frac{3\ m\ m_1\ k^{3/2}}{8(2\pi)^{1/2}\ n_1\ Z^2 Z_1^2\ e^4\ \ln \Lambda}\ \left(\frac{T}{m} + \frac{T_1}{T_1}\right)^{3/2}$	$3\ 10^3$	10^8	sec
" " " ($p^+ \alpha^{++}$)	. . . . .	100	10^6	sec
" " " ($e^- \alpha^{++}$)	. . . . .	$3\ 10^3$	10^8	sec
Interparticle distance	$r_2 = (2\ N_e)^{-1/3}$	$3\ 10^{-3}$	0.5	cm
Debye length	$r_D = \sqrt{\frac{k\ T}{4\pi\ e^2\ N_e}} = 6.9\ \sqrt{\frac{T\ [K]}{N_e\ [cm^{-3}]}}$ [cm]	3	10^3	cm
Larmor radius (e^-)	$r_L = \sqrt{\frac{8\ k\ T\ m}{\pi}}\ \frac{c}{ZeB} = 3.5\ 10^{-2}\ T^{1/2}/Z\ B\ [G]$ [cm]	100	$3\ 10^5$	cm
Larmor radius (p^+)	$r_L = 10\ v_T$ [km/sec] /Z B [γ] [cm]	$4\ 10^3$	$6\ 10^6$	cm
Mean free path (e^-)	$1 = t_D\ \sqrt{w^2 + v_T^2}$	$5\ 10^9$	$6\ 10^{13}$	cm
Mean free path (p^+)	. . . . .	$4\ 10^9$	$5\ 10^{13}$	cm

Density scale height	$H = \frac{k(T_e + T_p)}{2\mu\, m_H\, g}$ or $H = r/2$ (at 1 AU)	$3\ 10^{10}$	$7\ 10^{20}$	cm
Knudsen number (e^-)	$\mathcal{K} = \frac{\ell}{H}$	0.2	8	---
" " (p^+)	. . . . .	0.15	6	---
Beta (e^-)	$\beta = \frac{N k T}{B^2/8\pi} = 3.5\ 10^{-15}\ \frac{N\,[cm^{-3}]\ T\,[K]}{B^2\ [Gauss]}$	0.3	1	---
(p^+)	. . . . .	0.3	0.3	---
Magnetic Reynolds number	$\mathcal{R}_m = \frac{L w \sigma}{c^2}$; $\sigma = 2\ 10^7\ T^{3/2}$ [sec^{-1}]	$3\ 10^{12}$	$3\ 10^{14}$	---
Reynolds number	$\mathcal{R}_e = \frac{L\, o\, w}{\eta}$; $\eta = 1.2\ 10^{-16}\ T^{5/2}$	1	2	---
Prandtl	$\mathcal{P}_r = \frac{c_p\, \eta}{\kappa}$; $\kappa = 8.2\ 10^{-7}\ T^{5/2}$	1/43	1/43	---
Jeans number	$\lambda = \frac{G \mathcal{M} m_H}{2\ rk\ T} = \frac{1.14\ 10^7}{T\,[K]} \cdot (\frac{R_\odot}{r})$	3.8	0.56	---
Roche number	$\mathcal{R}_o = \frac{\Omega^2 r}{G\mathcal{M}/r^2} = 1.8\ 10^{-5}\ (r/R_\odot)^3$	$6\ 10^{-5}$	182	---